# Long-Period Wave Responses in a Harbor with Narrow Mouth

Weon Mu Jeong[1], Kil Seong Lee[2] and Woo Sun Park[1]

## Abstract

*Field measurements of long-period wave have been preformed for the Gamcheon Harbor in Korea. A Galerkin finite element model based on the extended mild-slope equation has been developed for simulating harbor oscillation more accurately. Infinite and joint elements are introduced to accomodate radiation condition at infinity and matching conditions at harbor mouth for the consideration of the energy loss due to flow separation, respectively. Comparisons with the results obtained by hydraulic experiments by Lepelletier (1980) show that the present model gives fairly good results. Model results reveal that the influence of entrance loss at the harbor mouth is considerably significant. From the application to the Gamcheon Harbor it is seen that the computed resonant periods and amplification ratios well agree with the measured results. The entrance loss effects were found to be insignificant unless the incident wave height is large.*

## Introduction

Long-period harbor oscillations could create unacceptable vessel movements leading to the downtime of moored ships. It is practically very difficult to prevent long-period harbor oscillations, but extension of breakwaters at the harbor mouth could be a countermeasure in part. Narrowing a harbor mouth might give rise to increase in the energy loss due to flow separation near the mouth, which in turn makes resonant periods of the harbor become longer, especially for the Helmholtz resonant mode. Referring to Lepelletier (1980), the reduction of a harbor mouth can reduce the amplification ratios of Helmholtz mode considerably.

[1]Senior Research Scientist, Coastal and Harbor Engineering Research Center, Korea Ocean Research and Development Institute, 1270 Sa-dong, Ansan, Kyeonggi-do, 425-170, Korea
[2]Professor, School of Civil, Urban and Geo-Systems Engineering, Seoul National University, San56-1, Sinrim-dong, Kwanak-ku, Seoul, 151-742, Korea

This study includes field measurements for short- and long-period waves around the Gamcheon Harbor in Korea, and the development of a finite element model based on the extended mild-slope equation, which incorporates the bottom frictional dissipation and the entrance loss due to flow separation. The present model can also handle the harbor resonance problems in a harbor with non-straight coastlines. The model is verified through the comparisons with Lepelletier (1980)'s experimental results. Finally, the model is applied to the Gamcheon Harbor with narrow mouth and compared with field measurements.

## Field Measurement

Field measurements for short- and long-period waves have been performed around Gamcheon Harbor which is located at the east-southern coast of Korea. The harbor is 4,000 m long, 1,150 m wide and has entrance of 240 m wide. In spite of narrow mouth, this commercial harbor is suffering from severe downtime problems in summer season. The measurement period was from November 27 to December 13 in 1997. Four pressure-type wave gauges (PWG), and one Aanderaa RCM-9 current meter were deployed at locations shown in Figure 1. Sampling intervals for the pressures at Sts. P1 and P4 were set to 5 seconds, while pressure data at Sts. P2 and P3 were gathered in the interval of 1 second. Current velocities from RCM-9 were averaged over 1 minute.

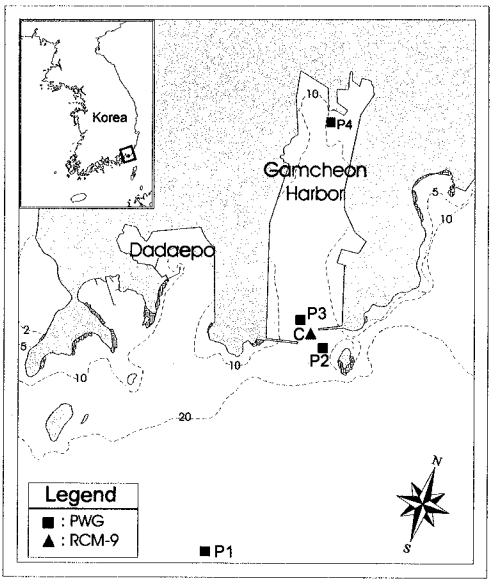


Figure 1. Location Map of Field Measurements.

After filtering tidal components from pressure signals using a Butterworth high-pass filter in MATLAB, spectral analyses of the 16 sets of filtered pressure data were performed. Figure 3 shows the power spectral densities of long-period wave data set no. 6 obtained at the four stations. We can find the first and second resonant modes appear near 2,000 seconds and 600~700 seconds, respectively. It is noted that the period of Helmholtz resonant mode of Gamcheon Harbor is 27.0~33.3 minutes, and the second and third resonant periods appear at 9.4~12.1 and 5.2~6.2 minutes, respectively. Figure 3 shows the power spectral densities of current velocity normal to the harbor mouth. It is noted that the maximum value appears around 28.2~31.9 minutes corresponding to the Helmholz mode.

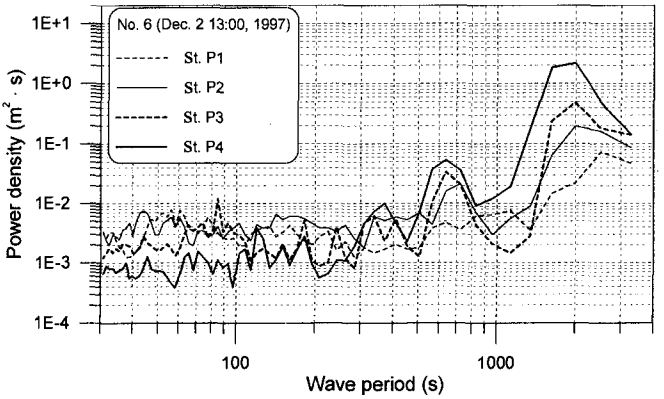


Figure 2. Power Spectral Densities Obtained at Sts. P1~P4.

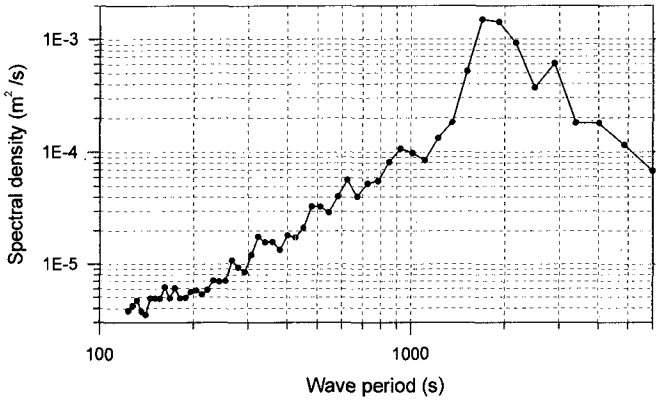


Figure 3. Power Spetral Densities for Observed Velocity at St. C.

## Galerkin Finite Element Model

### *Theoretical Formulation*

A Cartesian coordinate system ( $x$, $y$) and a cylindrical coordinate system ( $r$, $\theta$) are employed for mathematical formulation. The domain in the model is divided into two regions as shown in Figure 4. One is a near field region ( $\Omega_1$) that is modeled as conventional finite elements and the other is a far field region ( $\Omega_2$) that is represented as infinite elements of which shape functions satisfy the radiation condition at infinity. In the far field region, the water depth is assumed to be constant in the radial direction, but the depth in the circumferential direction varies with the value of the interface between the far and near field regions, $\Gamma_I$. To take into account the entrance loss at the narrow harbor mouth, the near field region is again divided into two sub-regions, that is inner ( $\Omega_{1i}$) and outer regions ( $\Omega_{1o}$) of the harbor (see Figure 4).

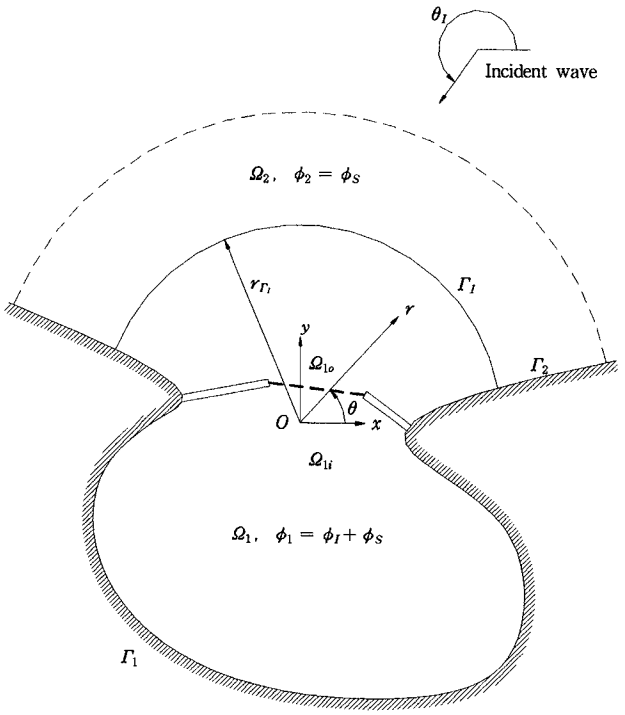


Figure 4. Definition Sketch for Boundary Value Problem.

The monochromatic and simple time harmonic waves propagating over a steeply sloped sea bed with variable depths in both regions may be described as follows (Massel, 1993; Suh et al., 1997).

$$\nabla \cdot (CC_g \nabla \phi_i) + \frac{C_g}{C} \omega^2 \phi_i - \omega^2 \{R_1 (\nabla h)^2 + R_2 \nabla^2 h\} \phi_i = 0 \tag{1}$$

in which $\nabla = (\partial/\partial x)\hat{i} + (\partial/\partial y)\hat{j}$, $\hat{i}$ and $\hat{j}$ are unit vectors in the directions of $x$ and $y$, respectively, $\phi_i$ is the two-dimensional spatial complex valued velocity potential, the subscript $i$ denotes the near field region for $i = 1$ and the far field region for $i = 2$, $\omega$ is the angular frequency, $h(x, y)$ is the water depth, $R_1$ and $R_2$ are coefficients for second-order bottom effects corresponding to the squared bottom slope $(\nabla h)^2$ and the bottom curvature $\nabla^2 h$ (see Suh et al., 1997). Wave celerity, $C$ and group velocity, $C_g$ are given as

$$C = \sqrt{\frac{g}{k} \tanh kh} \tag{2}$$

$$C_g = \frac{C}{2}\left(1 + \frac{2kh}{\sinh 2kh}\right) \tag{3}$$

in which $k$ is the wave number.

To consider the effects of wave absorbing, the partial reflection boundary condition is introduced along the solid boundaries, which was proposed by Mei and Chen(1975) as a function of an empirical reflection coefficient, $K_r$ normal to the solid boundaries. This boundary condition is represented as

$$\frac{\partial \phi_1}{\partial n} = \alpha \phi_1 \qquad \text{on } \Gamma_1 \tag{4a}$$

$$\frac{\partial (\phi_2 + \phi_I)}{\partial n} = \alpha (\phi_2 + \phi_I) \qquad \text{on } \Gamma_2 \tag{4b}$$

in which $\phi_1$ is the total velocity potential in the near field region, $\phi_2$ is the scattered wave potential in the far field region, $\phi_I$ is the incident wave potential, $n$ is outward normal to the solid boundary, and $\alpha$ is expressed as

$$\alpha = ik \cos\theta_I \frac{1 - K_r}{1 + K_r} \tag{5}$$

in which $\theta_I$ is the angle of the incident wave normal to the solid boundary.

The matching boundary condition on $\Gamma_I$ can be expressed as

$$\phi_1 = \phi_2 + \phi_I \tag{6a}$$

$$\frac{\partial \phi_1}{\partial n} = -\frac{\partial(\phi_2 + \phi_I)}{\partial n} \tag{6b}$$

The scattered wave potential, $\phi_2$ in the far field region must satisfy the Sommerfeld radiation condition at infinity.

$$\lim_{r\to\infty} \sqrt{r}\left(\frac{\partial \phi_2}{\partial r} - ik\phi_2\right) = 0 \tag{7}$$

The incident wave potential is given as

$$\phi_I = -\frac{igA_0}{\omega} e^{ikr\cos(\theta-\theta_I)} \tag{8}$$

in which $A_0$ is the amplitude of incident wave and $\theta_I$ is the attack angle of incident wave.

Two matching conditions were introduced on the interface boundary of two sub-regions, i.e., velocity and pressure continuity conditions at the harbor mouth (Unluata and Mei, 1975). For the entrance loss effects, the following matching conditions are introduced.

$$u_i = u_o \tag{9}$$

$$\frac{p_i}{\rho} = \frac{p_o}{\rho} + \frac{1}{2}\frac{f_e}{g} u_o|u_o| + \frac{l_j}{g}\frac{\partial u_o}{\partial t} \tag{10}$$

where, $u$ is the flow velocity, $p$ is the pressure, the subscript $i$ denotes the inner region and $o$ denotes the outer region, $\rho$ is the fluid density, $f_e$ is the loss coefficient and $l_j$ is the jet length. The quadratic non-linear energy loss term was linearized by using Lorentz transformation and equating depth averaged power, that is,

$$\frac{1}{2}\frac{f_e}{g} u_o|u_o| = \frac{1}{2}\alpha u_o \tag{11}$$

where, the linearized loss coefficient $\alpha$ is given by

$$\alpha = \frac{8}{9\pi}\frac{f_e}{g}\overline{u_o}\tanh kh \frac{5+\cosh 2kh}{2kh+\sinh 2kh} \tag{12}$$

where, $\overline{u_o}$ indicates the wave mean velocity.

In the above equations, $f_e$ and $l_j$ are determined by hydraulic experiments for various cross-sections. We used $f_e$ based on the inverse Strouhal number, $u_e/a\omega$ suggested by Lepelletier (1980). Then the linearized matching condition can be given by

$$\frac{\partial \phi_{1i}}{\partial n} = -\frac{\partial \phi_{1o}}{\partial n} \tag{13}$$

$$\frac{\partial \phi_{1i}}{\partial n} = \frac{1}{\frac{ia}{\omega} + \frac{l_j}{g}}(\phi_{1o} - \phi_{1i}) \tag{14}$$

in which $\phi_{1i}$ and $\phi_{1o}$ are complex velocity potentials of the inner and outer regions, respectively. For the jet length, a simple formula suggested by Morse and Ingard (1968) is used.

*Finite Element Formulation*

- Discretization of Fluid Domain

To discretize the fluid domain in the standard finite element manner, it is necessary to describe the unknown potential, $\phi_i$, in terms of the nodal potential vector, $\{\phi_i^e\}$, for an element $(e)$, and the prescribed shape function vector, $\{N\}$, as follows:

$$\phi_i = \{N\}^T\{\phi_i^e\} \tag{15}$$

Using Galerkin's technique, the boundary value problem can be re-formulated as integral equations. Using following definition of the residual for each element

$$\{R^e\} = -\int_{\Omega_i^e}\{N\}\left[\nabla\cdot(CC_g\phi_i) + \frac{C_g}{C}\omega^2\phi_i - \omega^2\{R_1(\nabla h)^2 + R_2\nabla^2 h\}\phi_i\right]d\Omega_i^e \tag{16}$$

and Green's second identity, and introducing the above boundary conditions, the system equation can be obtained for each element. Taking the residual as zero gives following simultaneous equations:

$$\sum_e^n\left\{\left([K^e_{\Omega_i}] + [K^e_{\Gamma_i}] + [K^e_{\Gamma_{mi}}]\right)\{\phi_i^e\} + \{F^e_{\Gamma_i}\} + \{F^e_{\Gamma_{Ii}}\} + \{F^e_{\Omega_i}\}\right\} = \{0\} \tag{17}$$

in which $[K^e_{\Omega_1}]$, $[K^e_{\Gamma_1}]$, $[K^e_{\Gamma_{m1}}]$, $\{F^e_{\Gamma_1}\}$, $\{F^e_{\Gamma_{I1}}\}$, and $\{F^e_{\Omega_1}\}$ are the element system matrices given by for the near field region:

$$[K^e_{\Omega_1}] = \int_{\Omega^e_1} \left[ CC_g \left( \left\{ \frac{\partial N}{\partial x} \right\} \left\{ \frac{\partial N}{\partial x} \right\}^T + \left\{ \frac{\partial N}{\partial y} \right\} \left\{ \frac{\partial N}{\partial y} \right\}^T \right) - \omega^2 \left( \frac{C_g}{C} - \{R_1(\nabla h)^2 + R_2 \nabla^2 h\} \right) \{N\}\{N\}^T \right] d\Omega^e_1 \tag{18a}$$

$$[K^e_{\Gamma_1}] = \int_{\Gamma^e_1} CC_g \alpha \{N\}\{N\}^T d\Gamma^e_1 \tag{18b}$$

$$[K^e_{\Gamma_{m1}}] = \int_{\Gamma^e_{m1i}} CC_g \frac{\partial \phi_{1i}}{\partial n} \{N\} d\Gamma^e_{m1i} + \int_{\Gamma^e_{m1o}} CC_g \frac{\partial \phi_{1o}}{\partial n} \{N\} d\Gamma^e_{m1o} \tag{18c}$$

$$\{F^e_{\Gamma_1}\} = \{0\} \tag{18d}$$

$$\{F^e_{\Gamma_{I1}}\} = - \int_{\Gamma^e_I} CC_g \frac{\partial(\phi_2 + \phi_I)}{\partial n} \{N\} d\Gamma^e_I \tag{18e}$$

and for the far field region:

$$[K^e_{\Omega_2}] = \int_{\Omega^e_2} \left[ CC_g \left( \left\{ \frac{\partial N}{\partial r} \right\} \left\{ \frac{\partial N}{\partial r} \right\}^T + \frac{1}{r^2} \left\{ \frac{\partial N}{\partial \theta} \right\} \left\{ \frac{\partial N}{\partial \theta} \right\}^T \right) - \omega^2 \left( \frac{C_g}{C} - \{R_1(\nabla h)^2 + R_2 \nabla^2 h\} \right) \{N\}\{N\}^T \right] d\Omega^e_2 \tag{19a}$$

$$[K^e_{\Gamma_2}] = \int_{\Gamma^e_2} CC_g \alpha \{N\}\{N\}^T d\Gamma^e_1 \tag{19b}$$

$$[K^e_{\Gamma_{m2}}] = 0 \tag{19c}$$

$$\{F^e_{\Gamma_2}\} = \int_{\Gamma^e_2} CC_g \left( \alpha \phi_I - \frac{\partial \phi_I}{\partial n} \right) \{N\} d\Gamma^e_2 \tag{19d}$$

$$\{F^e_{\Gamma_{I2}}\} = - \int_{\Gamma^e_I} CC_g \frac{\partial(\phi_1 - \phi_I)}{\partial n} \{N\} d\Gamma^e_I \tag{19e}$$

- Finite, Infinite and Joint Elements

The inner region is modeled by using three-noded triangular elements, in which the water depth $h$, the square of bottom slope $(\nabla h)^2$, and the curvature $\nabla^2 h$ are assumed to be constant for the convenience of numerical calculation. In order to model efficiently the radiation condition at infinity, a two-noded infinite element is developed. The shape function of the element is given by

$$\{N\} = N_r(\xi)\{N_\theta(\eta)\} \quad \text{for } 0 \le \xi \le \infty, \ -1 \le \eta \le 1 \tag{20a}$$

$$\{N\} = N_r(\xi) \quad \text{for } 0 \le \xi \le \infty \tag{20b}$$

in which $\{N_\theta(\eta)\}$ is the Lagrange shape function, and $N_r(\xi)$ is the shape function in the radial direction given by

$$N_r(\xi) = \frac{\sqrt{r_{\Gamma_I}}}{\sqrt{\xi + r_{\Gamma_I}}} e^{(ik-\varepsilon)\xi} \tag{21}$$

in which $\varepsilon$ is the artificial damping parameter( $\varepsilon < k$), and $r_{\Gamma_I}$ is the distance to the infinite elements from the origin as shown in Figure 4. The artificial damping parameter has been introduced to make the integration in Eq. (19e) in the radial direction bounded. After the integration is completed analytically, the value of $\varepsilon$ is taken to be zero. The shape function, $N_r(\xi)$, in the radial direction, except for the artificial damping parameter, have been derived from the asymptotic expression for the first kind of Hankel's function in the analytical boundary series solutions such as

$$\phi_S \propto \frac{1}{\sqrt{r}} e^{ikr} \tag{22}$$

The above shape functions satisfy the radiation condition at infinity.

- Matching the Inner and Outer Regions

Using the matching boundary conditions in Eq. (6), the total system matrices can be assembled as

$$\sum_e^n \left\{ ([K^e_\Omega] + [K^e_\Gamma])\{\phi^e_i\} + \{F^e_\Gamma\} + \{F_{\Gamma_I}\} \right\} = \{0\} \tag{23}$$

in which

$$[K^e_\Omega] = [\ K^e{}_{\Omega_1}], \quad [\ K^e{}_{\Omega_2}] \tag{24}$$

$$[K^e_\Gamma] = [\ K^e{}_{\Gamma_1}], \quad [\ K^e{}_{\Gamma_2}], \quad [\ K^e{}_{\Gamma_m}] \tag{25}$$

$$\{F^e_\Gamma\} = \{\ F^e{}_{\Gamma_2}\} \tag{26}$$

$$\{\ F^e{}_{\Gamma_I}\} = -\int_{\Gamma^e_I} CC_g \frac{\partial \phi_I}{\partial n}\{N\} d\Gamma^e_I - ([\ K^e{}_{\Omega_2}] + [\ K^e{}_{\Omega_2}])\{\phi^e_I\} \tag{27}$$

and $\{\phi_I^e\}$ is the vector of the incident wave potential corresponding to the nodal points.

## Numerical Analyses and Discussions

### *Verification of the present model*

To prove the validity of present model, numerical analyses have been performed for a rectangular harbor used by Lepelletier (1980) in hydraulic experiments. Two types of rectangular harbor have been tested. One is a fully open harbor ($a/b$ = 1.0, $a$ is width of a harbor entrance, $b$ is width of harbor) and the other is a partially open one ($a/b$ = 0.2). In Figures 6 and 7, numerical results without and with entrance losses are presented with the experimental results by Lepelletier (1980), respectively. As shown in figures, the calculated amplification ratios considering energy loss effects due to flow separation coincide very well with the experimental results. Neglecting energy loss effects obviously over-estimates the ratio.

In general, the length of jet-flow, $l_j$ has been taken to be zero. As the $l_j$ increases, the resonant periods move toward longer periods and amplification ratios at the resonant conditions increase. These phenomena have been confirmed in this verification. As shown in Figure 7, amplification ratios for the case with $l_j$ = 0.0284 m are smaller than those for the case with $l_j = 0$. This is due to shifting of the first resonant condition. The results considering the effects of the jet-flow are better fitted to the measured results. As mentioned before, the length of the jet-flow is estimated from the theoretical formula proposed by Morse and Ingard (1968) which was derived for the narrow channel with a thin gate. It may be required to develop a new formula for estimating the length of jet-flow at the harbor mouth more accurately.

### *Application of the present model*

To prove the applicability of the present model to the real case and to investigate the characteristics of long-period oscillations in a harbor with narrow mouth, numerical analysis was performed for the Gamcheon Harbor shown in Figure 1. As previously mentioned, field measurements were carried out using four PWGs and one RCM-9. For the direct comparison of the field measurements and calculated results, the informations for the incident waves such as wave heights and directions are estimated. However, it is nearly impossible to obtain the accurate informations from the limited set of field measurements, especially for long- period waves. Therefore, the incident wave angles were assumed to be equal to the main direction of short-period waves previously measured. A wave height for each wave frequency was determined from comparisons of the estimated and measured results at two stations, P1 and P2 at the outside of the

harbor. The estimated incident long-period wave heights were in the range of 0.03~0.07 m.

The amplification ratios at the innermost station, P4 are plotted in Figure 8. In this figure, hollow black circles indicate 13 measured data and black squares indicate the estimated results. The resonant periods and amplification ratios simulated by the present model are well agree with the measured results. To investigate the effects of the entrance losses in the real situation, the numerical analysis without considering the entrance losses was performed. The effects of the entrance losses were however almost insignificant in the whole tested range, except for the slight difference near the first resonant condition. This may be due to the fact that the incident wave heights are small in the present case. The entrance losses might be effective when the incident wave height is large as the case of attacking of tsunami.

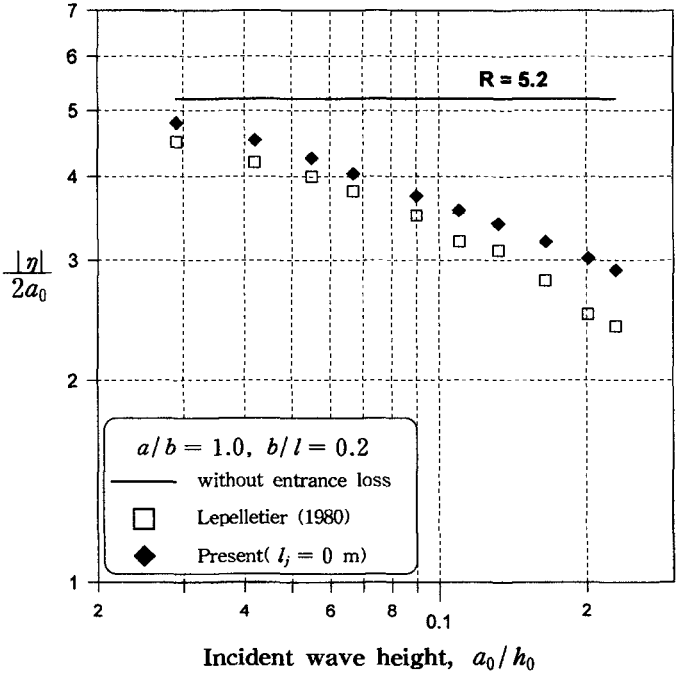


Figure 6. Variation in Amplification Ratios with respect to Incident Wave Heights for a Fully Open Rectangular Harbor ($a/b$ = 1.0).

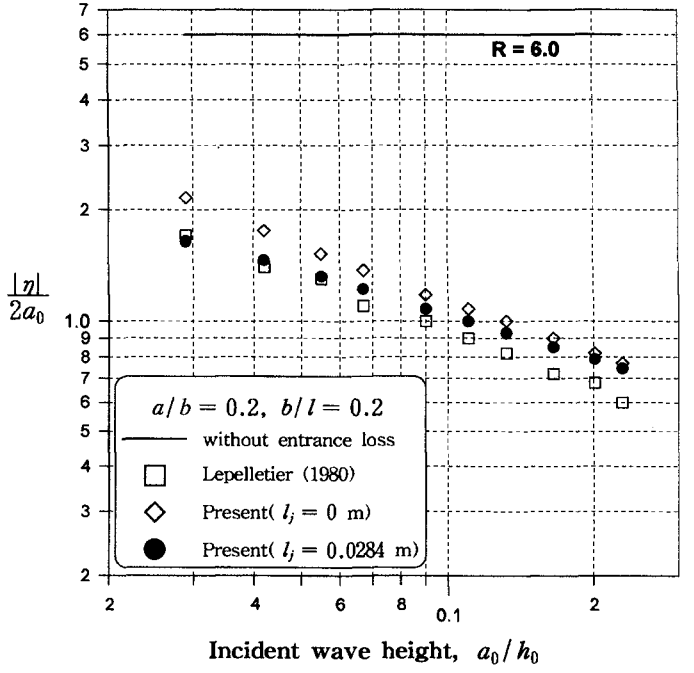


Figure 7. Variation in Amplification Ratios with respect to Incident Wave Heights for a Partially Open Rectangular Harbor ($a/b$ = 0.2).

## Conclusions

In this paper, the long-period wave oscillations in a harbor with narrow mouth has been studied. Field measurements were performed for a harbor with narrow mouth, Gamcheon Harbor in Korea. A Galerkin finite element model based on the extended mild-slope equation was developed which can handle the entrance losses due to flow separation. Verification of the present model was proved through the comparison of the estimated and experimental results. Comparisons of estimated and measured data in field shows that the present model gives quite reasonable results.

The effects of the entrance losses are insignificant unless the incident wave height is large. This may be true for tsunami. It was also found that strong jet-flow can affect the resonant condition, i.e., the resonant periods are moving toward longer period and amplification ratios are amplifying especially for the resonant conditions, as the jet-flow is being strong.

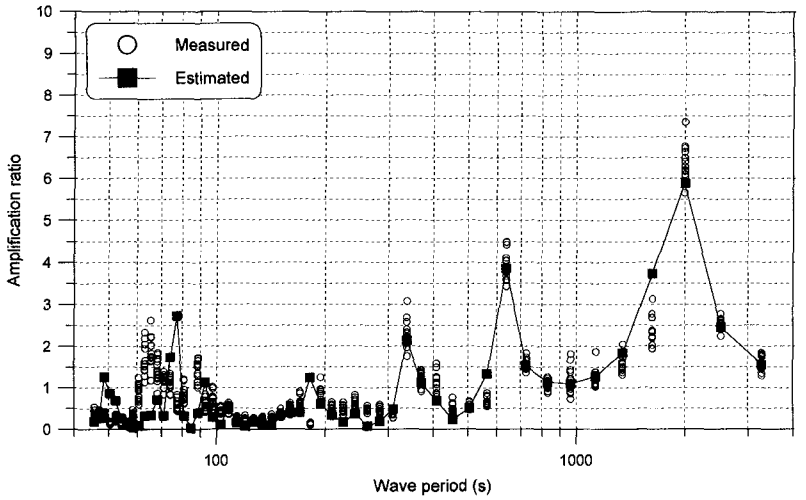


Figure 8. Comparison of Measured and Calculated Results for Gamcheon Harbor.

Acknowledgements

Partial support for this research was provided by Korea Ocean Research and Development Institute through Project Nos. BSPE 97625-00-1055-2 and BSPE 97608-00-1052-2. The authors would like to thank to their colleagues for providing field data.

References

Chen, H. S. (1986). "Effects of bottom friction and boundary absorption on wave scattering." *Applied Ocean Research*, Vol. 8, No. 2, pp. 99-104.

Jeong, W. M., Chae, J. W., Jun, K. C., Lee, J. C., and Cho, H. Y. (1997). *A study on the propagation of bound waves.* Korea Ocean Research and Development Institute, BSPE 97625-00-1055-2, 174 p. (in Korean).

Jeong, W. M., and Park, W. S. (1996). "Sensitivity analysis on hybrid element model for harbor oscillation." *J. Korean Society of Coastal and Ocean Engineers*, Vol. 8, No. 2, pp. 174-184. (in Korean).

Lepelletier, T. G. (1980). "Tsunamis - harbor oscillations induced by nonlinear transient long waves." *Report No. KH-R-41*, W. M. Keck Lab. of Hydrodynamics and Water Resources, CIT, Pasadena, C.A.

Liu, P. L.-F. (1986). "Effects of depth discontinuity on harbor oscillations." *Coastal Engrg.*, Vol. 10, pp. 395-404.

Massel, S. R. (1992). "Extended refraction-diffraction equation for surface waves." *Coastal Engrg.*, Vol. 19, pp. 97-126.

Morse, P. M., and Ingard, K. U. (1968). *Theoretical acoustics*. McGraw-Hill Inc., New York.

Suh, K. D., Lee, C., and Park, W. S. (1997). "Time-dependent equations for wave propagation on rapidly varying topography." *Coastal Engrg.*, Vol. 32, pp. 91-117.

Unluata, U., and Mei, C. C. (1975). "Effects of entrance loss on harbor oscillations." *J. of Waterways, Harbours and Coastal Engrg. Div.*, ASCE, Vol. 101, No. WW2, pp. 161-180.